Iraqi Journal of Natural Sciences and Nanotechnology IJNSN

Journal Homepage : https://publications.srp-center.iq/index.php/ijn

Highly Sensitive Flexible ZnO/PET Photodetector

Salah M. Saleh Al-Khazali[1]*, Husam S. Al-Salman[2], A. Hmood[3]

[1]The General Directorate for Education in Najaf, Ministry of Education, Najaf, Iraq.

[2,3]Department of Physics, College of Science, University of Basrah, Basrah, Iraq.

Corresponding author [1]**e-mail*: mm.salah47@gmail.com

Keywords:
ZnO;
Flexible UV Photodetector;
CBD Method;

Abstract

Current study involves fabricate a photodetector based on ZnO nanorods for ultraviolet sensing application deposited onto a low cost flexible substrate of polyethylene terephthalate (PET) using chemical bath deposition (CBD) method. XRD diffraction data approved hexagonal structure (Wurtzite). Nanorod structure of Zinc Oxide were noticed utilizing field emission scanning electron microscopy with an average diameter of 150 to 225 nm. The energy bandgap of 3.27eV were obtained using UV–Vis spectroscopy measurement. The maximum responsivity value was 0.023A/W at a wavelength of 375nm. The photosensitivity (Sph), quantum efficiency (η), response time, and recovery time were 1347.2, 837.53, 90.87s, and 114.57s under a UV light of 375nm at a bias voltage of 10V, respectively.

Introduction

The nanostructures based on flexible substrate have attracted great interested in the recent years. [1]. Flexible electronic devices exhibit special features and interface links with other components such as sensors of biomedical[2], electronics of organic, low-cost photovoltaic cells, [3] transistors[4]. Low-cost polyethylene terephthalate (PET) substrate has reactivity of low chemical, high resistivity and dielectric resistance across wide range of frequencies, which are consider the motiva ting points for the microelectronic applications[5]. In the last decade, a numerous researcher has been interested with flexible ultraviolet (UV) detectors using the ZnO nanostructure as active detection layer. Zinc oxide (ZnO) possesses a significantly large energy bandgap, denoted as Eg, measuring approximately 3.36 electron volts (eV), Additionally, a high exciton binding energy, is estimated to be over 60 (meV), nontoxic, inexpensive, and available in abundance, and ease of synthesis with various morphologies[6]. Numerous manufacturing techniques have been commonly used to produce ZnO nanorods (NRs) including chemical vapor deposition, epitaxy of molecular beam, pulsed laser deposition[6], [7], sol-gel, hydrothermal, chemical bath deposition (CBD)[3], [8]. One of the approaches utilized in this study

 DOI: https://doi.org/10.47758/ijnsn.v5i1.113

is the chemical bath deposition (CBD), which is a straightforward and cost-effective process employed for the manufacture of ZnO NRs on a (PET) substrate, with the aim of facilitating UV sensing applications.

Experimental procedure

Utilized The CBD method was used to synthesize ZnO NRs onto PET substrate. The PET substrate was ultrasonically cleaning with deionized water (DI), acetone, ethanol, and again with DI with 10 minutes for each, then dry it in air flow. After dissolving 0.1M $Zn(CH_3COOH)_2.2H_2O$ in ethanol and stirring for 20 hours at room temperature, a clear, homogeneous solution was obtained. A Spin coating technique was used to achieve a homogeneous seed layer, where the prepared solution was poured onto PET substrate with 3500 rpm utilizing a dropper for 36s, then heated at 130 $°C$ for 4min. The aforementioned procedure was iterated for a total of Saven instances. The seed layer was thereafter subjected to an annealing process for a duration of 1.25 hours at a temperature of 170 $°C$. The ZnO/PET seed layer was vertically suspended in a solution consisting of equimolar concentrations of $Zn(NO_3).6H_2O$) and ($C_6H_{12}N_4$) in deionized water (DI) at a temperature of 94 $°C$ for a duration of 2 hours. This article summarizes the chemical events that occur during ZnO NRs production on various substrates [9]:

$$C_6H_{12}N_4 + 6H_2O \rightarrow 6HCHO + 4NH_3$$
$$NH_3 + H_2O \rightarrow NH_4^+ + OH^-$$
$$2OH^- + Zn^{2-} \rightarrow Zn(OH)_2$$
$$Zn(NO_3)_2 \rightarrow Zn^{2+} + 2NO_3^-$$
$$Zn(OH)_2 \rightarrow ZnO + H_2O$$

By allowing the ($C_6H_{12}N_4$) complex to decompose thermally, OH^- anions could be introduced into the solution, controlling the reaction's kinetics. In addition, presence of ZnO seed layer leads to quick nucleation process. These factors could affect the energy of activation between the substrate and ZnO crystal layers. [8]

The thin film of vertically aligned ZnO NRs was subjected to annealing at a temperature of 180℃ for a duration of 2 hours. To complete the fabrication of the flexible ZnO/PET detector, aluminum comb-like electrodes were deposited onto the ZnO/PET using a thermal evaporation process (Fig. 1a and b). The structure and morphology were characteristics by SIEMENS D500 X-ray diffractometer and FEI NOVA SEM 450 provided with an EDX system to investigate the stoichiometric ratio of the ZnO/PET. A Shimadzu-1650 UV-Vis spectrometer was utilized to analyze the optical properties. Current-voltage (I-V) characterization under UV wavelengths of 405, 385, and 375 nm were calculated using a source meter (Keithley-2430) connected to a personal computer (PC) for data processing purposes.

 DOI: https://doi.org/10.47758/ijnsn.v5i1.113

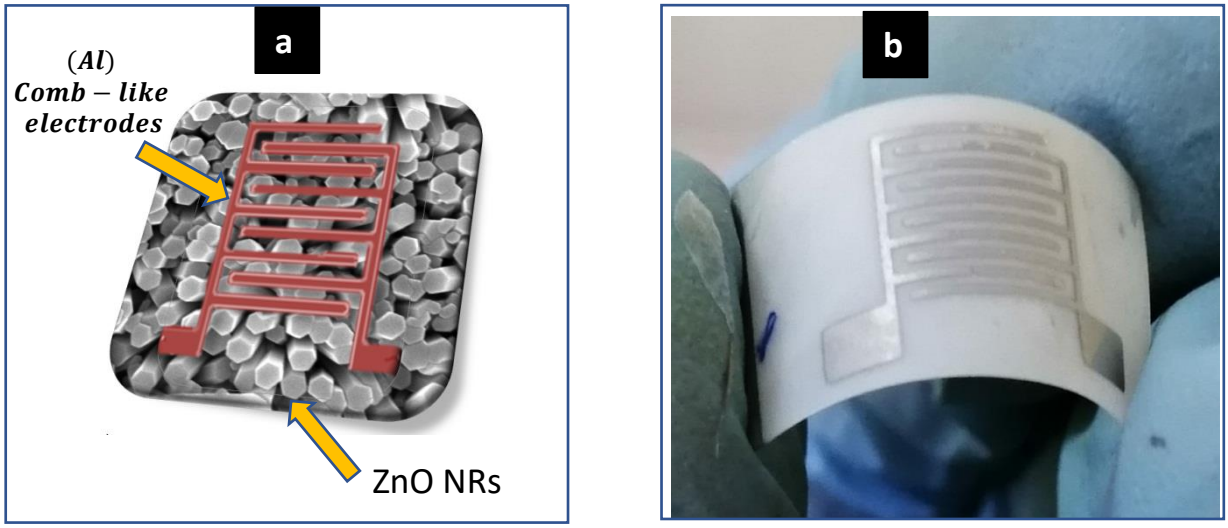

Figure 1. (a) Schematic diagram of Al comb-like electrodes onto the ZnO/PET NRs; (b) Real image of the ZnO/PET photodetector.

Results and discussion

Crystal structure and surface morphology: Figure 2 illustrated the XRD pattern of the ZnO NRs film which reveal the polycrystalline with hexagonal wurtzite phase with dominant orientation of (002), which matches to JCPDS card No. 36-1451. [8], [10]. The full width at half maximum FWHM, β, of (002) peak was 0.179, which indicate a good crystalline quality. The peaks at 2θ of 26.03o, 47.46o, and 53.74o in Fig. 2, were assigned to the PET substrate. [11]. The size of crystallite, D, was determined employing Debye-Scherrer formula. [8].

$$D = \frac{0.9\lambda}{\beta \cos\theta} \qquad (1)$$

where λ: is the wavelength and Θ: is Bragg diffraction angle. The size of crystallite was decided to be 46.48nm. The strain, ε_{zz}, is directly dependent on the lattice constant c and its value, which is a criteria of crystal quality, could be determined by the following relation. [3], [8]:

$$\varepsilon_{zz} = \frac{|c_{ASTM} - c_{XRD}|}{c_{ASTM}} \times 100 \qquad (2)$$

Where cXRD and cASTM were the c-lattice constant which matches to XRD pattern and the ASTM card, respectively. The calculated ε_{zz} value was 0.16. Figure 3(a) illustrate the surface morphology of ZnO/PET photodetector.

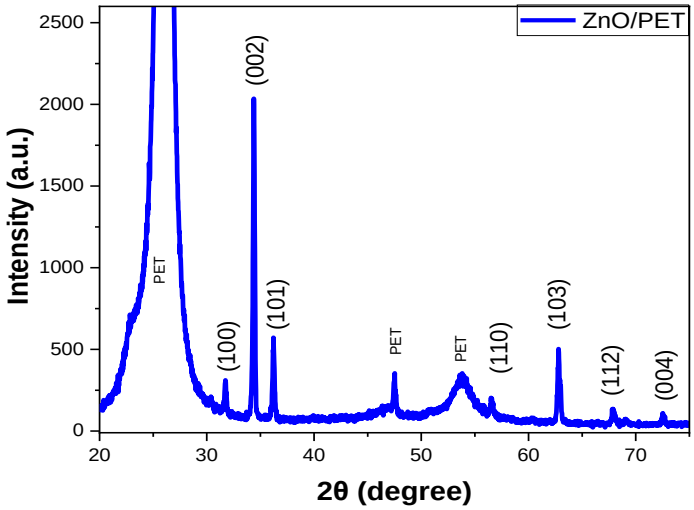

Figure 2. shows ZnO nanorods on a PET flexible substrate by X-ray diffraction.

The ZnO was grew as nanorods with a uniform distribution, homogenous, hexagonal morphology and vertically alignment onto the PET polyester. The average nanorods diameter estimated to be between 150 and 225 nm, as display in Fig. 3(b). The height of the ZnO NRs was determined to be 2.98 μm based on the cross-sectional analysis, as depicted in Fig. 3(c). Figure 3(e) reveals the peaks in the EDX spectrum, which have been identified as carbon (arising from PET polyester), oxygen, and zinc. The carbon element results from the PET polyester.

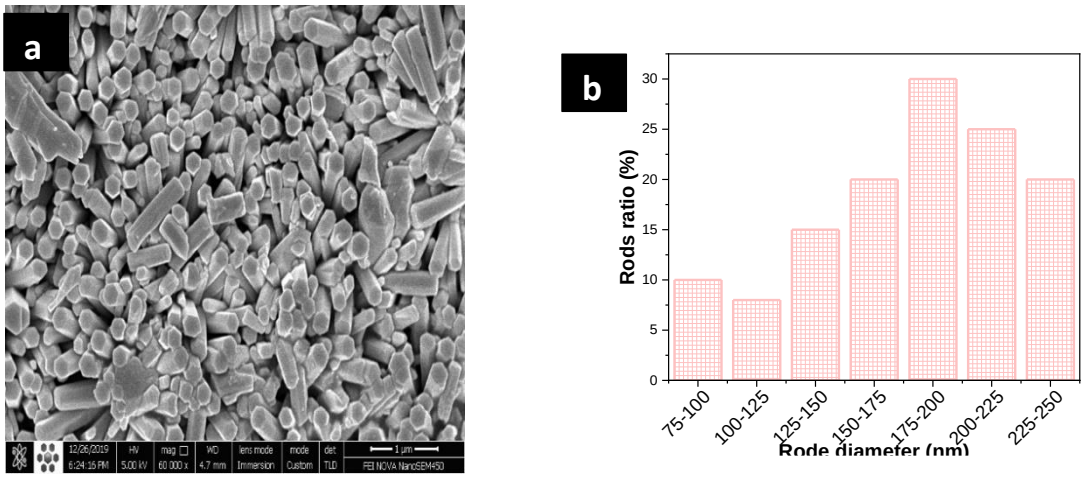

©SRP 2024, DOI: https://doi.org/10.47758/ijnsn.v5i1.113

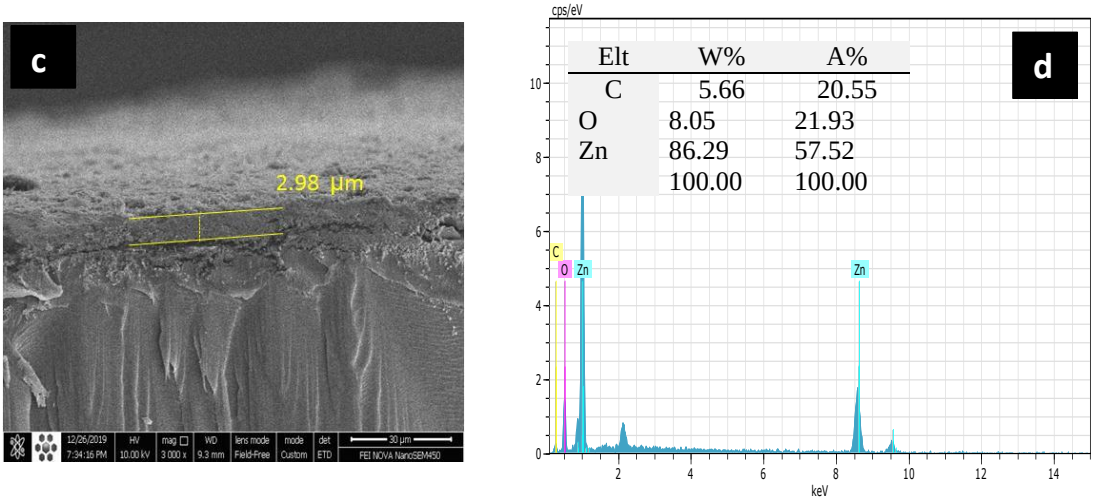

Figure 3. displays the surface morphology of the film dependent on ZnO NRs; (a) FESEM image; (b) diameter histogram distribution; Panel (c) showcases a cross-sectional view, and panel (d) exhibits the EDX spectrum.

Optical properties: The absorption spectrum of ZnO NRs on PET substrate illustrated in Fig. 4(a). High absorbance was observed in the ultraviolet range, exhibiting a distinct threshold at a wavelength of around 378nm. The essential absorption of ZnO NRs film attributed to the permitted direct transitions, which given by [3], [6]:

$$\alpha h\upsilon = A_{\alpha}(h\upsilon - Eg)^{1/2} \qquad (3)$$

Where hν is the incident photon energy, α is the absorption coefficient, Eg is the energy bandgap and Aα is the parameter associated with transition probability. By plotting (αhν)2 vs hν, Fig. 4(b), the calculated Eg was 3.27eV. This value is well agreement with previous results. [3], [6], [8].

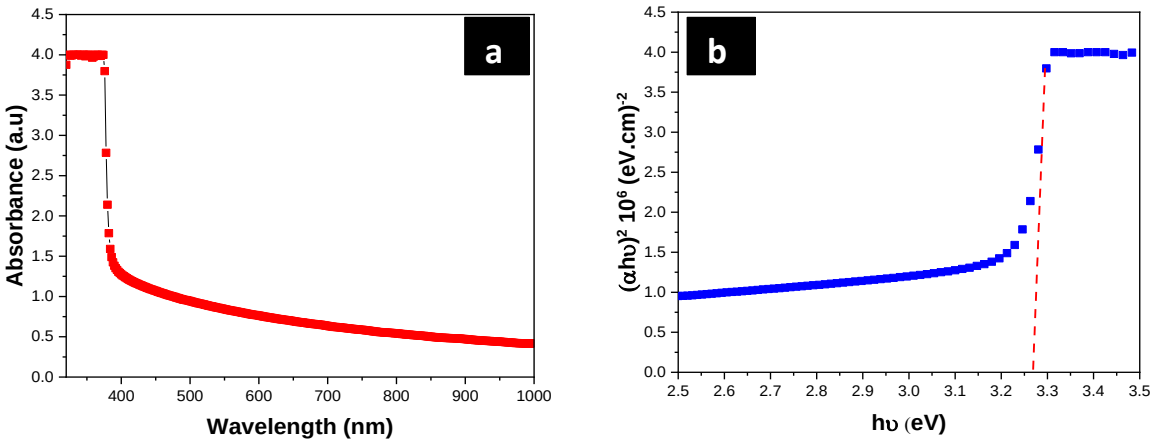

©SRP 2024, DOI: https://doi.org/10.47758/ijnsn.v5i1.113

Figure 4. Optical properties of the film dependent on ZnO NRs: (a) The absorbance spectrum; (b) Plot of $(\alpha hv)2$ vs. hv.

Photodetector Characteristics: The spectral response considered a significant photodetector parameter which determines the detection efficiency at a Specific wavelength. The responsivity, R_λ, is provided by [12]:

$$R_\lambda = \frac{I_{ph}(A)}{P_{in}(W)} \qquad (4)$$

where I_{ph} and P_{in} were photocurrent and incident photon power, respectively. Fig. 5(a) depicts the spectral response of the ZnO/PET PD under 5V bias voltage. Increasing the wavelength to 375nm leads to increase the responsivity to 0.023A/W, which is decreases with further increasing the wavelength. This value was higher than reported previously. [13]. Fig. 5b shows the I–V curves under dark and 375, 385, and 405 nm wavelength illuminations with incident power of 50 µW/cm2, 40 µW/cm2 and 0.45 mW/cm2, respectively. I–V curves reveals the ohmic behavior of the detector. The photocurrent of 375nm was higher those obtained from 385 and 405nm.

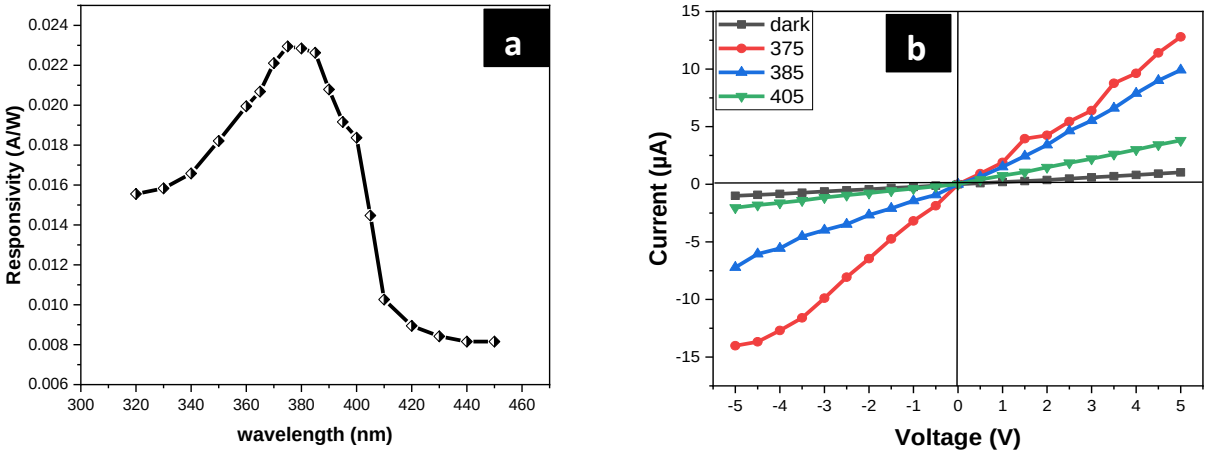

Figure 5. (a) Spectral response of ZnO/PET detector at 5 V bias; (b) The I–V characteristics in the dark and under UV wavelength.

Figure 6(a-c) illustrates the photocurrent dependent of the interval time $(I-t)$at a bias voltage of 5 and 10V with ON/OFF UV wavelengths lighting of 375, 385, and 405nm. Under 10V bias, the photocurrent gain (I_{ph}/I_{dark}) under a UV wavelength illumination of 375, 385, and 405nm were 14.47, 11.93, and 3.49, compared with 12.4, 9.61, and 3.69, respectively; under 5V bias. Fig. 6(d) depicts the $(I-t)$ curve under various UV wavelengths for several cycles under 10V bias. These results revealed high stability, repeatability, and reproducibility of the ZnO/PET PD. The photosensitivity (Sph) and quantum efficiency (η) of the detector achieved using the following relationships. [6]

$$S_{ph}(\%) = (\frac{I_{ph}-I_{dark}}{I_{dark}}) \times 100 \quad (5)$$

$$\eta\,(\%) = [\frac{I_{ph}}{q}\frac{hv}{P_{in}}] \times 100 \quad (6)$$

where I_{dark}, v, q and h are the dark current, incident photon frequency, electric charge, and Planck constant, respectively. Based on Fig. 6 and equations (4) and (5), the calculated photodetector properties were listed in Table (1).

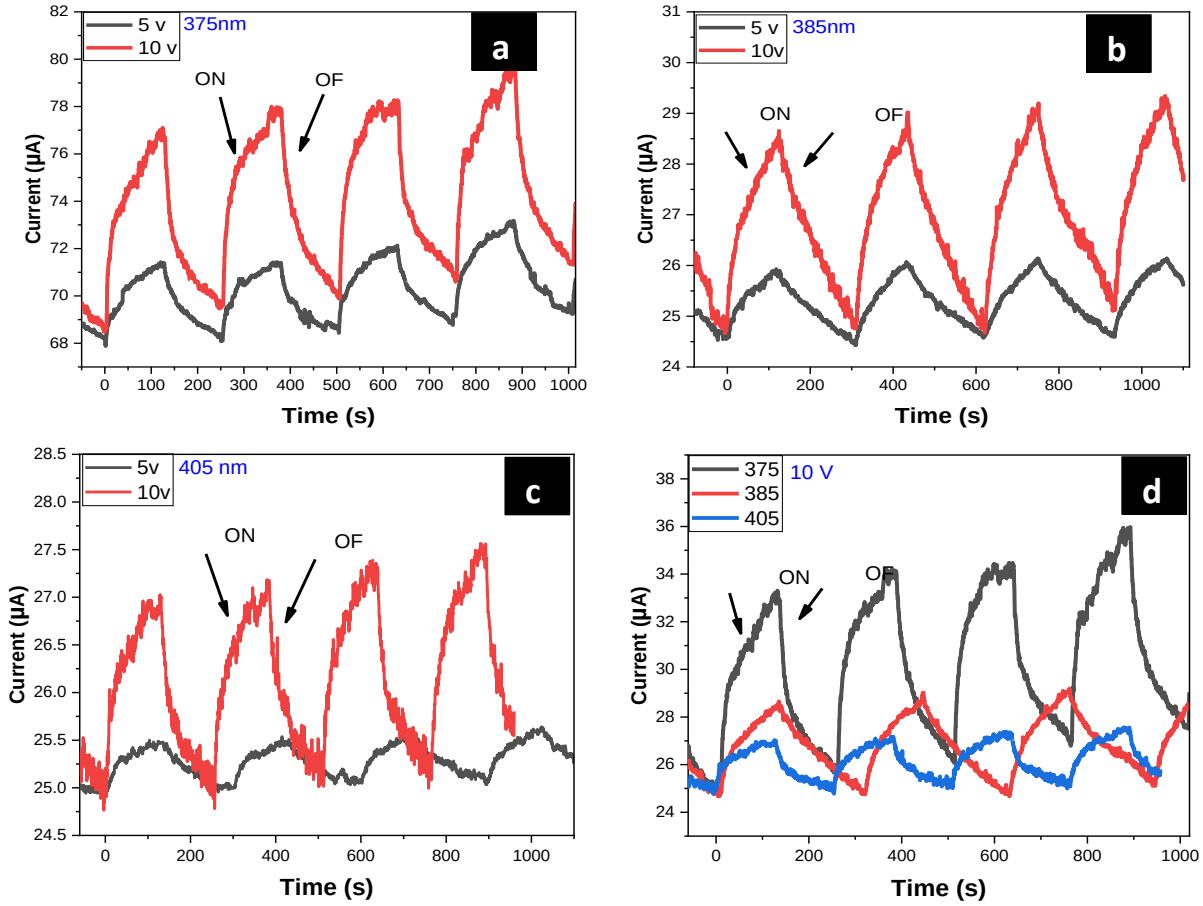

Figure 6. Photocurrent response spectra as a function of time under ON/OFF UV wavelength of 375, 385, and 405nm with various bias voltages.

The value of photosensitivity for ZnO/PET PD under 375 nm light was 1140.8 and 1347.2 at 5 and 10V bias respectively, were higher than that obtained from 385 and 405 nm. These results were better than previously published. [10], [14], [15]. Generally, the quantum efficiency values under 10V bias were higher than those of 5V bias for all wavelength, and its maximum value was 837.53 under 375nm light, Table 1. The response time, denoted by the symbol τRes, is defined as the amount of time that elapses before the Iph current reaches 90%

©SRP 2024, DOI: https://doi.org/10.47758/ijnsn.v5i1.113

of its maximum value. The recovery time, denoted by the symbol τRec, refers to the amount of time that elapses before the *Ip*h current falls to 10% of its maximum value. Both times were obtained using Fig. 6(a-d). For 375nm wavelength, the estimated values of τRes were 89.83 and 90.87s and τRecwere113.37 and 114.57s under 5 and 10V bias respectively. However, Table (1) shows the short recovery and response times under 405 nm compared with 375 and 385 nm light, which might attribute to the high intensity of 405 nm wavelength (0.45 mW/cm2). In additions, Table (1) explain that the τRec is comparatively longer than the τRes, which resulted by the carrier's slow relaxation time in the deep defect state and the interspaces between the ZnO NRs. [16].

Table 1- ZnO/PET Photodetector properties under various UV wavelength exposure.

Bias voltage (V)	Wavelength (nm)	τ*R*es (s)	τ*R*ec (s)	I_{ph} (μA)	I_{dark} (μA)	Gain	Quantum efficiency %	Photosensitivity%
5	375	89.83	113.37	12.793	1.031	12.4	311.14	1140.8
	385	*92.55	134.32	9.913		9.61	286.06	861.49
	405	*83.64	105.35	3.81		3.69	7.56	269.54
10	375	*90.87	114.57	34.011	2.35	14.47	837.53	1347.2
	385	94.96	145.97	28.04		11.93	827.14	1093.1
	405	77.83	92.30	8.216		3.49	15.96	249.61

Conclusion

The ZnO NRs deposited onto PET flexible substrate employing CBD technique was investigated. The structural and morphology characterizations showed that the ZnO possessed hexagonal wurtzite polycrystalline structure that vertically well alignment onto PET substrate. The results showed high stability of the ZnO/PET PD over the time with photosensitivity of 1347.2% toward UV wavelength of 375nm under 10V bias with quantum efficiency of 837.53%. The photosensitivity toward 375nm was high compared with those obtained toward 385 and 405nm. The exceptional performance of the potential flexible photodetector can be attributed to the nanorods' high surface-to-volume ratio.

Acknowledgements

The authors express their sincere gratitude for the financial support provided by the Department of Physics, College of Science, University of Basrah, located in Basrah, Iraq.

References

[1] M. Y. Zhang, Q. Nian, and G. J. Cheng, 'Room temperature deposition of alumina-doped zinc oxide on flexible substrates by direct pulsed laser recrystallization', Appl Phys Lett, vol. 100, no. 15, Apr. (2012).
[2] A. Arena, N. Donato, G. Saitta, A. Bonavita, G. Rizzo, and G. Neri, 'Flexible ethanol sensors on glossy paper substrates operating at room temperature', Sens Actuators B Chem, vol. 145, no. 1, pp. 488–494, Mar. (2010).
[3] S. M. Saleh Al-Khazali, H. S. Al-Salman, and A. Hmood, 'Low cost flexible ultraviolet photodetector based on ZnO nanorods prepared using chemical bath deposition', Mater Lett, vol. 277, p. 128177, Oct. (2020).
[4] J. A. Hauch, P. Schilinsky, S. A. Choulis, R. Childers, M. Biele, and C. J. Brabec, 'Flexible organic P3HT:PCBM bulk-heterojunction modules with more than 1 year outdoor lifetime', Solar Energy Materials and Solar Cells, vol. 92, no. 7, pp. 727–731, Jul. (2008).
[5] M. G. Faraj, K. Ibrahim, and A. Salhin, 'Fabrication and characterization of thin-film Cu (In, Ga) Se2 solar cells on a PET plastic substrate using screen printing', Mater Sci Semicond Process, vol. 15, no. 2, pp. 165–173, Apr. (2012).
[6] H. S. Al-Salman and M. J. Abdullah, 'Preparation of ZnO nanostructures by RF-magnetron sputtering on thermally oxidized porous silicon substrate for VOC sensing application', Measurement, vol. 59, pp. 248–257, Jan. (2015).
[7] W. Chebil, A. Gokarna, A. Fouzri, N. Hamdaoui, K. Nomenyo, and G. Lerondel, 'Study of the growth time effect on the structural, morphological and electrical characteristics of ZnO/p-Si heterojunction diodes grown by sol-gel assisted chemical bath deposition method', J Alloys Compd, vol. 771, pp. 448–455, Jan. (2019).
[8] S. M. Saleh Al-Khazali, H. S. Al-Salman, A. Hmood, A. H. Omran Alkhayat, and S. M. Thahab, 'NO<inf>2</inf> Gas Sensing Performance Based on ZnO Nanorods Synthesized by Chemical Bath Deposition Technique', in AIP Conference Proceedings, (2022).
[9] N. T. Son, J. S. Noh, and S. Park, 'Role of ZnO thin film in the vertically aligned growth of ZnO nanorods by chemical bath deposition', Appl Surf Sci, vol. 379, pp. 440–445, Aug. (2016).
[10] Y.-L. Chu et al., 'Fabrication and Characterization of UV Photodetectors with Cu-Doped ZnO Nanorod Arrays', J Electrochem Soc, vol. 167, no. 2, p. 027522, Jan. (2020).
[11] Q. Xie, X. Liu, and H. Liu, 'Fastly steady UV response feature of Mn-doped ZnO thin films', Superlattices Microstruct, vol. 139, p. 106391, Mar. (2020).
[12] S. I. Inamdar, V. V. Ganbavle, and K. Y. Rajpure, 'ZnO based visible–blind UV photodetector by spray pyrolysis', Superlattices Microstruct, vol. 76, pp. 253–263, Dec. 2014, doi: 10.1016/J.SPMI.2014.09.041.
[13] P. S. Shewale, S. H. Lee, and Y. S. Yu, 'Effects of annealing temperature of spin-coated ZnO seed-layer on UV photo-sensing properties of PLD grown ZnO: Mg thin films', J Alloys Compd, vol. 774, pp. 461–470, Feb. (2019).
[14] H. J. Lee et al., 'Facile synthesis of ZnO microrod photodetectors by solid-state reaction', J Alloys Compd, vol. 825, p. 154110, Jun. (2020).

[15] S. Liu et al., 'Self-Powered, Flexible Ultraviolet Photodetector Based on ZnO/Te All Nanowires Heterojunction Structure', physica status solidi (a), vol. 220, no. 5, p. 2200612, Mar. (2023).
[16] F. H. Alsultany, Z. Hassan, and N. M. Ahmed, 'A high-sensitivity, fast-response, rapid-recovery UV photodetector fabricated based on catalyst-free growth of ZnO nanowire networks on glass substrate', Opt Mater (Amst), vol. 60, pp. 30–37, Oct. (2016).